Mesenchymal Stem Cell Exosomes Induce Proliferation and Migration of Normal and Chronic Wound Fibroblasts, and Enhance Angiogenesis In Vitro

Arsalan Shabbir, Audrey Cox, Luis Rodriguez-Menocal, Marcela Salgado, and Evangelos Van Badiavas

Although chronic wounds are common and continue to be a major cause of morbidity and mortality, treatments for these conditions are lacking and often ineffective. A large body of evidence exists demonstrating the therapeutic potential of mesenchymal stem cells (MSCs) for repair and regeneration of damaged tissue, including acceleration of cutaneous wound healing. However, the exact mechanisms of wound healing mediated by MSCs are unclear. In this study, we examined the role of MSC exosomes in wound healing. We found that MSC exosomes ranged from 30 to 100-nm in diameter and internalization of MSC exosomes resulted in a dose-dependent enhancement of proliferation and migration of fibroblasts derived from normal donors and chronic wound patients. Uptake of MSC exosomes by human umbilical vein endothelial cells also resulted in dose-dependent increases of tube formation by endothelial cells. MSC exosomes were found to activate several signaling pathways important in wound healing (Akt, ERK, and STAT3) and induce the expression of a number of growth factors [hepatocyte growth factor (HGF), insulin-like growth factor-1 (IGF1), nerve growth factor (NGF), and stromal-derived growth factor-1 (SDF1)]. These findings represent a promising opportunity to gain insight into how MSCs may mediate wound healing.

Introduction

N ONHEALING CHRONIC WOUNDS represent a major healthcare burden, with an incidence of 6.5 million cases annually in the United States and an estimated $25 billion each year on treatment alone [1]. Unfortunately, approximately half of these chronic wounds do not respond to existing treatments [2].

The wound healing response requires a complex cascade of molecular and cellular events including cellular migration, proliferation, angiogenesis, extracellular matrix deposition, and tissue remodeling [3–5]. In contrast, chronic nonhealing wounds exhibit decreased production of growth factors and chemokines [6], reduced angiogenesis [7], decreased proliferation and reduced migration of fibroblasts [8,9], and an impaired inflammatory response [10].

Mesenchymal stem cells (MSCs) are self renewing multipotent stem cells derived from the bone marrow stroma and other tissues, which can differentiate into various lineages including bone, cartilage, and fat [11]. In addition to their multipotent potential, MSCs have an extensive ex vivo expansion capacity and can regulate immune and inflammatory processes, making these cells attractive for the treatment of numerous disorders [12]. MSCs have been shown to correct delayed wound healing in diabetic mice by promoting epithelialization, and augmenting angiogenesis and granulation tissue formation [13]. Furthermore, studies have shown that application of MSCs to nonhealing wounds can lead to increased angiogenesis and reduced scarring [14].

Interestingly, these results do not support MSCs differentiating to replace damaged tissue. Instead it is believed that MSCs exert their therapeutic effects by secreting soluble or ''paracrine'' factors that augment endogenous repair and regenerative mechanisms [15–18]. Also, work in our laboratory has found that MSCs can enhance fibroblast migration, an integral component of the wound healing process, without direct contact, suggesting the importance of paracrine signaling between these cells [19]. However, the exact molecular mechanisms of this correction are not clear.

Exosomes are small membrane-bound vesicles (diameter 30–120 nm), are secreted by a myriad of cells types and found in essentially all biological fluids, and originate from inward budding of late endosomes with resultant multivesicular bodies that are fused with the plasma membrane [20,21]. Furthermore, exosomes can shuttle transcription factors and genetic materials (mRNA and miRNA), implicating their role in cell-to-cell communication and modulating the molecular activities of recipient cells [22,23].

In this study, we hypothesized that MSC-derived exosomes play a significant role in wound healing. To test this, we

Department of Dermatology and Cutaneous Surgery, Interdisciplinary Stem Cell Institute, University of Miami Miller School of Medicine, Miami, Florida.

examined MSC exosomes, including their characterization, their effect on dermal fibroblasts (derived from both normal and chronic wounds) and endothelial cells, and we tried to deduce possible mechanisms that underlay these effects.

Materials and Methods

Cell lines

Human MSCs were isolated and expanded from normal donor bone marrow acquired from AllCells LLC (Emeryville, CA, www.allcells.com). Three different donors were used for these experiments. MSCs were isolated by the plastic adherence method as described in a previous study and found to be positive for CD105, CD90, CD73, HLA-Class-1, negative for CD45, and able to differentiate into osteogenic, chondrogenic and adipogenic lineages [19]. Stocks of low passage cells (passage <5) were also cryopreserved until use.

Diabetic wound patient fibroblasts were isolated from the wound edge and collected under a University of Miami IRB approved protocol (HSRO 20080299). Experiments were repeated from diabetic wound fibroblasts. Fibroblasts were collected from a 59-year-old male with uncontrolled diabetes who had a nonhealing ulcer of >2 years duration that had not healed despite standard of care and advanced wound care treatments. Normal adult fibroblasts were obtained from Lonza (Walkersville, MD). Cells were grown until 80%–90% confluence was reached and then passaged at a 1:4 to 1:6 ratios into new tissue culture flasks. Dermal fibroblasts were grown in FB media [Dulbecco's Modified Eagle Medium, 5% fetal bovine serum (FBS), and 1% Pen/Strep and 1% glutamine].

Coculture

For all cell labeling experiments, 1×10^6 cells were resuspended in 1 mL of α-MEM and incubated with 5 μL of 1 mM Vibrant Dil (MSCs) or Vibrant DiO (normal adult fibroblast) solution (Life technologies, Carlsbad, CA) for 20 min at 37°C in the dark followed by two wash steps in medium. Cocultures of labeled MSCs and normal adult fibroblasts were performed in monolayer at 50:50 ratios in fibronectin-coated four-well Nunc Lab-Tek II Chamber Slide system for 24 h in MSC media. Images were captured with an inverted IX81 Olympus microscope (Olympus America, Center Valley, PA) and ORCA-AG Hamamatsu digital camera (Hamamatsu Photonics K.K., Hamamatsu City, Shizuoka Pref., Japan) using red (for Dil) and green (for DiO) fluorescence microscopy.

MSC exosome purification and fluorescent labeling

FBS used in culture media for exosome isolation was precleared by ultracentrifugation in Beckman pollyallomer tubes (Beckman Coulter, Brea, CA) using the Optima L-XP preparative ultracentrifuge (Beckman Coulter) at 100,000 g for 3 h at 4°C as described by others [24]. It was subsequently filtered using a 0.22 μM filter (Corning, Corning, NY) (depleted FBS). BM-MSCs were grown in MSC media containing α-MEM, 20% depleted FBS, 1% penicillin/streptomycin, and 1% glutamine. Low passage (<5) BM-MSCs were grown to 60%–80% confluence in 5-layer 875 cm² multi-flasks (~17×10^6 to 22×10^6 MSCs per flask)

before isolation. Fresh BM-MSC media was layered and collected after 48 to 72 h (conditioned medium).

Exosomes were isolated by the ultracentrifugation protocol described by Théry et al. [25]. Briefly, hMSCs were conditioned in exosome-free medium for 48–72 h. The conditioned medium was transferred to 50-mL centrifuge tubes (Thermo Fisher Scientific, Rockford, IL) and centrifuged at 2,000 g at 4°C for 20 min to remove cells. The supernatant was carefully removed subsequently transferred to new 50-mL centrifuge tubes and centrifuged for 30 min at 10,000 g and 4°C to remove cellular debris. The supernatant was carefully removed and transferred to Beckman Optiseal™ polypropylene tubes and ultracentrifuged at 100,000 g at 4°C for 70 min with the Beckman Ti70 rotor using the Optima L-XP preparative ultracentrifuge. The supernatant was carefully removed and saved (Depleted conditioned medium) and the pellets were resuspended in 1 mL phosphate buffered saline (PBS). The pellets from all tubes were pooled and ultracentrifuged again at 100,000 g at 4°C for 70 min. The pellet was again washed in PBS and a final ultracentrifuge step was performed at 100,000 g at 4°C for 70 min. The final pellet was resuspended in 100 μL PBS. Recovered exosome protein contents were determined using the Pierce BCA protein assay kit (Thermo Fisher Scientific) per manufacturer's protocol. Exosomes were used immediately or stored at −70°C until use. Supernatant remaining after ultracentrifugation was also collected, filtered via a 0.22 μM filter, and stored at −70°C until use (depleted medium). For all experiments, depleted medium was used at a concentration of 10 μg/mL.

PKH26 labeling of exosomes

Exosomes were labeled with PKH26 (Sigma-Aldrich, St. Louis, MO) according to the manufacturer's protocol. Briefly, 7.5 mg of exosomes were resuspended in 1 mL of diluent C (Sigma-Aldrich) and mixed with PKH26 diluted in Diluent C for a final concentration of 2×10^{-6} M PKH26. The exosome-dye suspension was incubated for 5 min with regular mixing. Excess dye from the labeled exosomes were removed by centrifugation and resuspended in PBS (for a total of three washes) in 100k Amicon Ultra Centrifugal Filters-100k tubes (Millipore, Billerica, MA). A mixture without exosomes was used as a negative control to examine any carryover of PKH26 dye. For the negative control, labeling was performed as described but without exosomes.

Electron microscopy

Exosome pellets were deposited on Formvar carbon-coated electron microscopy (EM) grids and allowed to air dry. They were fixed with 2% gluteraldehyde, counterstained with 4% uranyl acetate, and visualized using the JEOL 1400 transmission electron microscope (JEOL USA, Peabody, MA). All electron microscopy was completed with assistance from the Electron Microscopy Core facility at the University of Miami.

Immunoblotting

MSCs and exosomes were lysed using RIPA containing 1 mM PMSF and protease inhibitors. After lysis, protein concentrations were measured using Pierce BCA protein assay kit. Cellular lysates and exosomal lysates were

subjected to SDS-PAGE and transferred to a PVDF membrane (BioRad Laboratories, Hercules, CA). PVDF membranes were incubated with a 1,000-fold diluted primary antibody solution overnight at 4°C. Washed membrane was probed with a horseradish peroxidase-conjugated secondary antibody at a 1:10,000 dilution. Signals were developed using the SuperSignal West Femto Chemiluminescent substrate from Pierce Biotechnology and imaged by Biorad's ChemiDoc system. Membranes were incubated with the following antibodies: CD-9, CD-81, CD-63, Hsp-70 (System Biosciences, Mountain View, CA), Alix, Flotillin-1, GM-130, Beta-Actin, GAPDH, phosphorylated Tyr705 of STAT3, total STAT3, phosphorylated Ser473 of Akt, total Akt, phosphorylated Thr202/204 of ERK1/2, total ERK1/2 (Cell Signaling, Danvers, MA), and Tsg-101 (Novus Biologicals, Littleton, CO).

STAT3 DNA binding

Cellular and exosomal extracts (10 µg) were assayed for STAT3 DNA binding activity using the TransAM kit (Active Motif, Carlsbad, CA) per manufacturer's instructions.

Cell proliferation

Fibroblasts were seeded at a density of 5×10^3 cells/well in 24-well plates in FB media. After overnight plating, an MTT assay (3-[4.5-Dimethylthiazol-2-yl]-2.5-diphenyltetrazolium bromide; Life technologies) was performed to obtain baseline values (day 0). MTT assay is a colorimetric assay that measures the chemical reduction of MTT into formazan, which is directly proportional to the number of viable cells. Cultures were incubated for 20 min in FB medium with 0.5 mg/mL of MTT. The resulting formazan was then extracted with DMSO and the optical density was measured at 540 nm. After obtaining day 0 values, wells were randomly selected to be treated with MSC exosomes (0.1, 1, and 10 µg/mL), vehicle (PBS), or depleted media (10 µg/mL). After 3 days of treatment, MTT assay was again performed (day 3).

Cell migration

For migration studies, $\sim 3 \times 10^5$ fibroblasts were seeded per well in six-well plates in FB media and maintained at 37°C and 5% CO_2 for at least 24 h to permit cell adhesion and the formation of a confluent monolayer. To inhibit the influence of cell proliferation, cells were treated with fresh serum-free culture medium containing mitomycin at 10 µg/mL. The confluent monolayer was then scored with a 1 mL sterile pipette tip. Culture medium was immediately removed (along with dislodged cells) and replaced with a fresh serum-supplemented culture medium containing MSC exosomes (0.1, 1, and 10 µg/mL), vehicle (PBS), or depleted media (10 µg/mL). Images were taken after the scratch and 16 h post treatment with the IX81 Olympus microscope. Three fields were analyzed per well using ImageJ software (http://rsbweb.nih.gov/ij/). All scratch assays were performed in triplicate.

Quantitative real-time polymerase chain reaction

For gene expression studies, fibroblasts were seeded in six-well plates in FB media and maintained at 37°C and 5% CO_2 for at least 24 h to permit cell attachment. After serum starvation overnight, cells were treated with MSC exosomes or vehicle for 24 h. RNA extraction from fibroblasts was performed using Qiagen RNeasy Mini Kit (Germantown, MD) per manufacturer's instructions. Three hundred nanograms of RNA was reverse transcribed to cDNA using iScript Reverse Transcription Supermix for quantitative real-time polymerase chain reaction (qRT-PCR) (BioRad Laboratories). PCR was performed using the Biorad CFX96 Real-Time PCR Detection System (BioRad Laboratories) machine with the SsoAdvanced SYBR Green Supermix (Bio-Rad). Amplification conditions after an initial denaturation step for 90 s at 95°C were 40 cycles of 95°C, 10 s, for denaturation, 55°C, 10 s, for annealing and 72°C, 30 s, for elongation. CFX96 manager software was used to determine threshold cycles. GAPDH was used as the reference gene for calculations. Data were analyzed by the 2ΔΔCT threshold cycle method. Oligonucleotides were synthesized by Integrated DNA Technologies (Coralville, IA). Primer sequences are listed in Table 1.

Tube formation assay

Angiogenesis was measured using an endothelial tube formation assay kit (Invitrogen Life Technologies, Grand Island, NY) per manufacturer's instructions. Briefly, human umbilical vein endothelial cells (HUVECs) were plated at a density of 5×10^4 cells/well in Geltrex coated 24-well tissue culture plates. Cells were treated with MSC exosomes (0.1, 1, and 10 µg/mL), vehicle (PBS), and depleted media (10 µg/mL). Treated cells were incubated for 6 h in 200PRF media

TABLE 1. Oligonucleotide Primers

Gene	Forward	Reverse	Amplicon length
GAPDH	CTCCTGTTCGACAGTCAGCC	ACCAAATCCGTTGACTCCGAC	101
C-myc	TAGTGGAAAACCAGCAGCCTCC	CGTCGCAGTAGAAATACGGCT	108
Cyclin A1	GCACCCTGCTCGTCACTTG	CAGCCCCCAATAAAAGATCCA	74
Cyclin D2	GCCACCGACTTTAAGTTTGCC	GCTCAGTCAGGGCATCACAA	127
HGF	CACGAACACAGCTTTTTGCC	CCCCTCGAGGATTTCGACAG	76
IGF1	TCTTGAAGGTGAAGATGCACAC	ACTGAAGAGCATCCACCAGC	135
IL-6	CTCATTCTGCCCTCGAGCC	GACCGAAGGCGCTTGTTGGA	97
ILRA	CCTCAGAAGACCTCCTGTCCT	GTCGGCAGATCGTCTCCTTTG	123
NGF	CACACTGAGGTGCATAGCGT	AGTGTGGTTCCGCCTGTATG	85
SDF1	AGATTGTAGCCCGGCTGAAG	GTGGGTCTAGCGGAAAGTCC	134
VEGF	GGGCCTCCGAAACCATGAA	GGGACCACTTGGCATGGTG	87

supplemented with 0.2% LSGS (limiting medium) at 37°C and 5% CO_2. At the end of incubation, HUVECs were stained with Calcein AM fluorescent dye for visualization of tube formation. Fluorescent images were captured with the inverted IX81 Olympus microscope and ORCA-AG Hamamatsu digital camera. Tube length was measured using NIH's Image J software (http://imagej.nih.gov/ij/).

Statistical analysis

Pairwise one-tailed Student's *t*-tests or one-way analysis of variance with Bonferroni's post hoc test were used in this study and the error bars are shown as standard error of the mean. Statistical significance was set at $P < 0.05$.

Results

Formation of a nanotubular network and secretion of microvesicles during coculture of fibroblasts and MSCs

To examine the transfer and determine the identity of possible transmitted cellular components, we used the lipophilic fluorophores, DiI (red fluorescence) and DiO (green fluorescence). These dyes will label plasma membranes, including exosomes, by stably inserting their hydrocarbon chains in to lipid bilayers. Both DiI and DiO are not cytotoxic and are known not to leak. MSCs were labeled with DiI and fibroblasts were labeled with DiO. The two populations were cocultured in a 1:1 ratio for 24 h. Live cell imaging revealed a nanotubular network among DiO-labeled fibroblasts (green) and DiI-labeled MSCs (red) after 24 h of coculture (Fig. 1A, B). In addition, we found that vesicle structures that appear to be consistent with microvesicle (MV) morphology (which have been found range in size from 50 nm to 1,000 nm) were found to be actively shed from both fibroblasts and MSCs. MSC MVs (red) were also found to be internalized by the DiO-labeled fibroblasts (Fig. 1C).

Characterization of MSC exosomes

To isolate and further characterize the MVs observed in Fig. 1, we employed an established isolation protocol described by Théry et al. that utilizes differential sedimentation to isolate exosomes, a type of microvesicle that has recently gained attention as being the possible paracrine mediators of MSCs (see Materials and Methods section) [25]. Electron microscopic analysis of the vesicles isolated by ultracentrifugation indicated a cup-shaped morphology with diameters approximately ranging between 30 and 100 nm (Fig. 2A) with an appearance similar to those reported from other cell lines [26–28]. An extensive biochemical profiling of exosomes was performed by western blot analysis (Fig. 2B) with a panel of antibodies, including those directed against exosomal marker proteins such as the tetraspanins (CD9, CD63, and CD81), proteins involved in multivesicular body biogenesis (Alix and Tsg101) and membrane transport and fusion (flotillin-1) [29]. As expected, CD9, CD81, Alix, TSG101, and flottilin-1 were strongly enriched in exosome preparations compared with cell lysates. We confirmed the presence of CD63 in exosomes. CD63 was, however, also detected in MSC cell lysate, but this was not unexpected as CD63 is expressed by MSCs [30]. Additionally, HSP70, β-actin, and glyceraldehyde-3-phosphate dehydrogenase were found in exosomes, typical of exosomes produced by varied cell types [31]. Further, the cis-golgi matrix protein gm130 was readily detected in cell lysates but was not found in exosomes, indicating that no contaminating cellular debris was present in the exosome preparations.

We next examined whether MSC-derived exosomes could be transferred to dermal fibroblasts. PKH26 fluorescently labeled exosomes isolated from MSC conditioned medium were cocultured with fibroblast cells overnight. After incubation with exosomes overnight at 37°C, cells were washed thrice and stained with Calcein AM. Live cell imaging revealed PKH26-labeled exosomes to be observed inside the Calcein-labeled fibroblasts, and they were mainly located in the perinuclear region (Fig. 2C), as reported by others [32–34].

MSC exosomes enhance normal and diabetic wound fibroblast growth

To explore whether MSC exosomes could induce the growth of fibroblasts, both normal adult and diabetic wound fibroblasts were incubated with vehicle (PBS), depleted

FIG. 1. Normal human mesenchymal stem cells (MSCs) and normal human fibroblasts form a nanotubular network and secrete microvesicles in coculture. **(A, B)** A nanotube network (*white arrows*) was observed among DiO-labeled fibroblasts (*green*) and DiI-labeled MSCs (*red*) after 24 h of co-culture. **(B)** Microvesicles were also shed into the culture medium, including evidence of cellular internalization (*white arrows*). Color images available online at www.liebertpub.com/scd
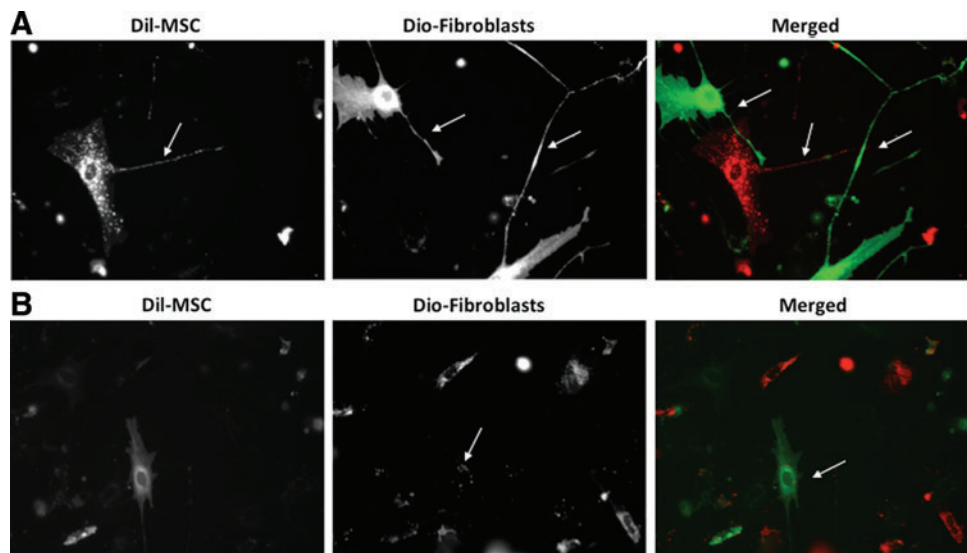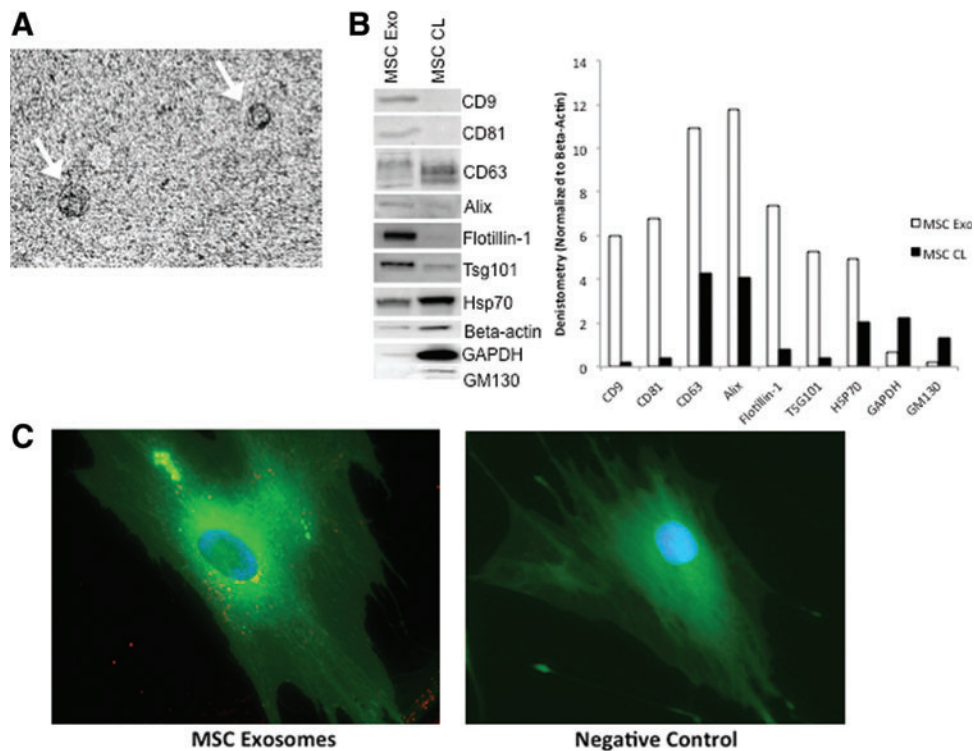
FIG. 2. Characterization of MSC exosomes. **(A)** Morphological characterization of exosomes isolated from MSCs by transmission electron microscopy at $130,000\times$ magnification. On scanning electron microscopy, exosomes had a cup-shaped morphology (*white arrows*). Densitometry of the bands normalized to Beta-Actin are shown on the *right hand side*. **(B)** Western blot analysis was performed as described in the Materials and Methods section. Twenty micrograms exosome and cellular extract preparations were loaded into the respective lane. Exosome preparations were found to be enriched for the exosomal markers CD9, CD63, CD81, Alix, Flottilin-1, and TSG101 while negative for GM130, a protein found in Golgi apparatus (GM130) and present in the cells lysates. **(C)** Purified exosomes were labeled with the dye pkh26 and added to cultures of fibroblasts. After incubation with exosomes overnight at 37°C, cells were washed thrice and stained with Calcein AM. Nuclei were counterstained with Hoechst 33342. Numerous pkh26 labeled MSC exosomes (*red*) were observed inside the fibroblasts (*left panel*), mostly located at the perinuclear region. On the *right panel*, a mixture without exosomes was used as a negative control to examine any carryover of PKH26 dye. Color images available online at www.liebertpub.com/scd

medium (10 μg/mL), and MSC exosomes at three different concentrations (0.1, 1.0, and 10 μg/mL) for 72 h. Normal adult fibroblast growth, as measured by the MTT assay, was found to be significantly increased and in a dose-dependent manner as compared to vehicle and depleted medium at day 3 (Fig. 3A).

The growth rate of diabetic wound fibroblasts was found to be significantly diminished compared with normal adult fibroblasts (Fig. 3B). A similar dose dependence response was noted when diabetic wound fibroblasts were treated with MSC-derived exosomes; however, it appeared that only the higher concentration of exosomes (10 μg/mL) was significant, compared to the vehicle and depleted medium, in inducing growth. This could be indicative of a blunted ability to respond to growth signals beyond that observed with growth factors.

MSC exosomes enhance normal and diabetic wound fibroblast migration

We next studied MSC exosomes in their ability to induce dermal fibroblast migration during the wound-healing process by using the scratch assay method, an in vitro procedure used to study cell migration [35]. Normal dermal fibroblasts

and diabetic wound fibroblasts were plated to confluence (at 3×10^5 cells/well in a six-well plate). After creation of the scratch, cells were treated with vehicle, depleted medium (10 μg/mL), and MSC exosomes (0.1, 1.0, and 10 μg/mL) for 16 h. The migration rate of normal adult fibroblasts after MSC exosome was found to be significantly increased at all doses as compared to vehicle and depleted medium (Fig. 4A, B). Further, a dose-response was noted with the 10-μg/mL dose demonstrating the greatest migration rate. Similar to normal adult fibroblasts, the migration rate of diabetic wound fibroblasts was significantly increased with MSC exosomes compared with vehicle and depleted medium (Fig. 4C). Interestingly, the maximal effect of MSC exosomes on the migration of diabetic wound fibroblasts was reached at 1 μg/mL, reflecting an enhanced sensitivity of diabetic wound fibroblasts. Hence, MSC exosomes were able to enhance the migration rate of normal and diabetic wound fibroblasts.

Endothelial cells internalize MSC exosomes during tube formation

Since endothelial cells play an important role in neovascularization and the wound healing process, we next determined the effects of MSC exosomes on the
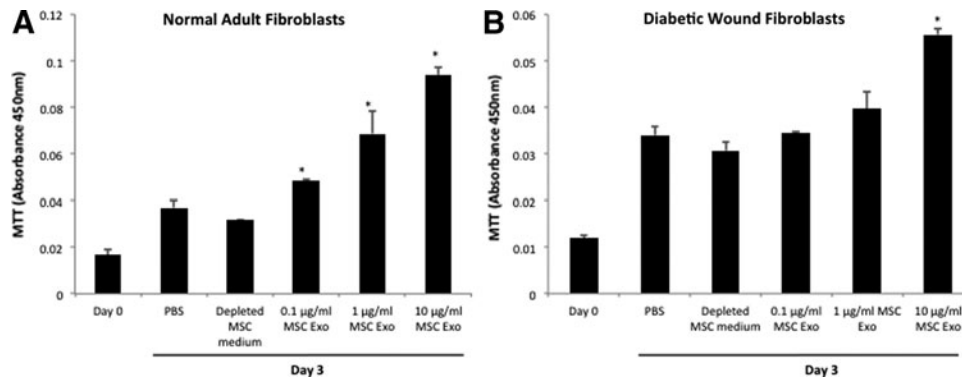
FIG. 3. MSC exosomes enhance growth of normal and diabetic wound fibroblasts. **(A, B)** Normal and diabetic wound fibroblasts were plated overnight (day 0) and were subsequently treated with different concentrations of MSC exosomes (0.1, 1, or 10 μg/mL), vehicle or depleted conditioned medium. Exosomes were isolated as described in the Material and Methods section. Supernatant remaining after ultracentrifugation was also collected, filtered via a 0.22 μM filter, and used at a concentration of 10 μg/mL (depleted MSC medium). MTT assay was performed at day 0 and after 3 days of treatment (day 3). MSC exosomes enhanced the proliferation of normal and diabetic wound fibroblasts over vehicle and depleted conditioned medium and in a dose-dependent manner. Each bar represents the mean ± standard error of the mean (SEM) of three independent experiments. *$P < 0.05$ versus vehicle day 3. Pairwise one-tailed Student's t-tests was used for statistical analysis.
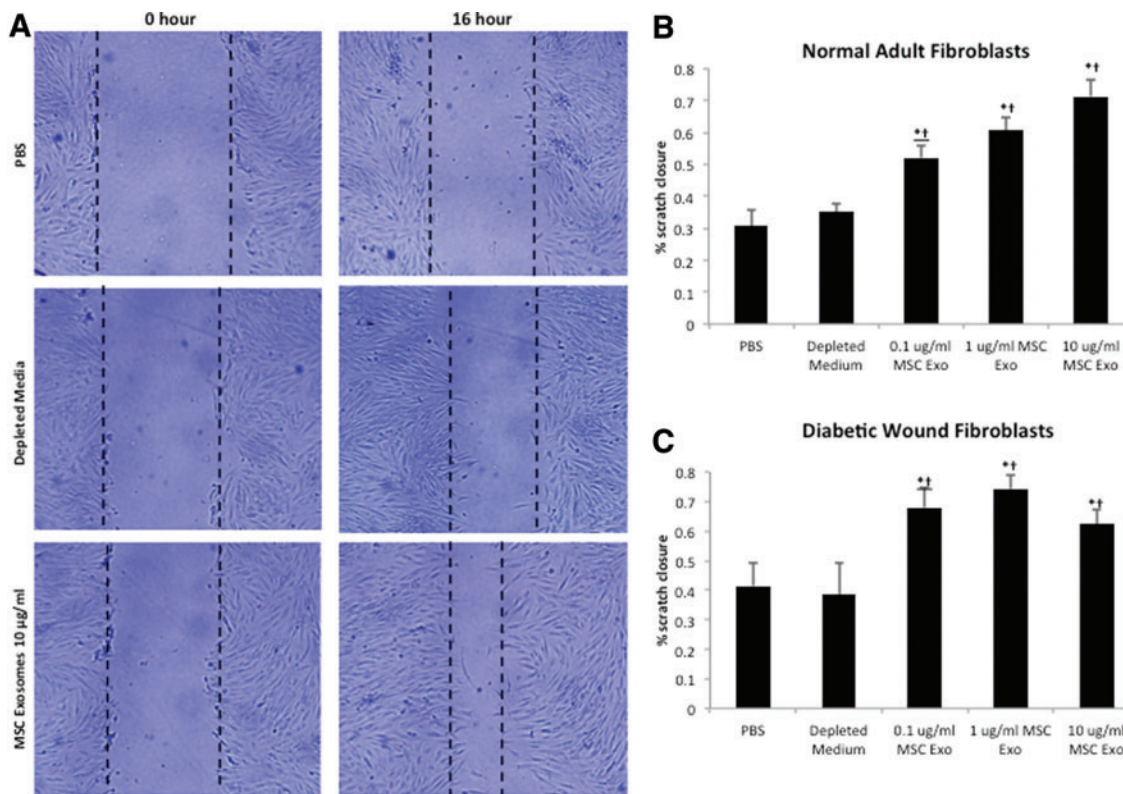

FIG. 4. MSC exosomes enhance the migration of normal and diabetic wound fibroblasts. Fibroblasts were plated to 100% confluency, treated with 10 μg/mL mitomycin for 2 h to inhibit the influence of proliferation, and mechanically "wounded" by scraping with a 1,000 μL Fisher-brand pipette tip. Cell monolayers were washed with phosphate buffered saline (PBS), imaged and subsequently treated with different concentrations of MSC exosomes (0.1, 1, or 10 μg/mL), vehicle or depleted conditioned medium. **(A)** Representative photomicrograph of the wound edge in the scratch assay at 0 and 16 h after MSC exosome, vehicle, and depleted medium. MSC exosomes significantly enhanced migration compared with vehicle and depleted conditioned medium. MSC exosomes enhanced the migration of normal **(B)** and diabetic wound fibroblasts **(C)** in a dose-dependent manner. Migration rates for MSC exosome treated fibroblasts were significantly greater than vehicle and depleted conditioned medium. The migration rate is represented at percent scratch closure. Each bar represents the mean ± SEM of three independent experiments. *$P < 0.05$ versus vehicle; [†]$P < 0.05$ versus depleted conditioned medium. Pairwise one-tailed Student's t-tests was used for statistical analysis. Color images available online at www.liebertpub.com/scd

behavior of cultured HUVECs. We first determined whether MSC exosomes could be uptaken by HUVECs. PKH26 fluorescently labeled MSC exosomes were incubated with HUVECs cultured on matrigel for 6 h under tube formation conditions (2% v/v LSGS-supplemented Medium 200PRF). After incubation with MSC exosomes, cells were washed thrice with PBS and stained with Calcein AM. Numerous small, granular PKH26-labeled MSC exosomes (red) were noted within the tubular network of HUVECs (green) (Fig. 5A). Hence, endothelial cells can internalize up MSC exosomes.

MSC exosomes induce vascular tube formation in vitro

We next hypothesized that MSC exosomes could induce tubular differentiation of HUVECs in vitro. HUVECs plated on Geltrex in limiting medium (0.2% v/v LSGS-supplemented Medium 200PRF) with increasing concentrations of

MSC exosomes formed an extensive tubular network in a dose-dependent manner (Fig. 5B, C). Furthermore, MSC exosomes were found to form greater tube formation compared with controls (vehicle and depleted medium) at all dosages. Depleted medium had a small, yet statistically significant, ability to induce tubular formation compared with vehicle.

MSC exosomes activate several intracellular signaling pathways and induce expression of cell cycle genes and growth factors

We next characterized the effects of MSC exosomes on intracellular signaling in normal dermal fibroblasts by examining the activation of AKT, ERK 1/2, and STAT3. These signaling pathways are known to be play critical roles in wound healing, including roles in cell proliferation, migration, and angiogenesis [36–38]. Normal adult fibroblasts were serum starved overnight and subsequently exposed to
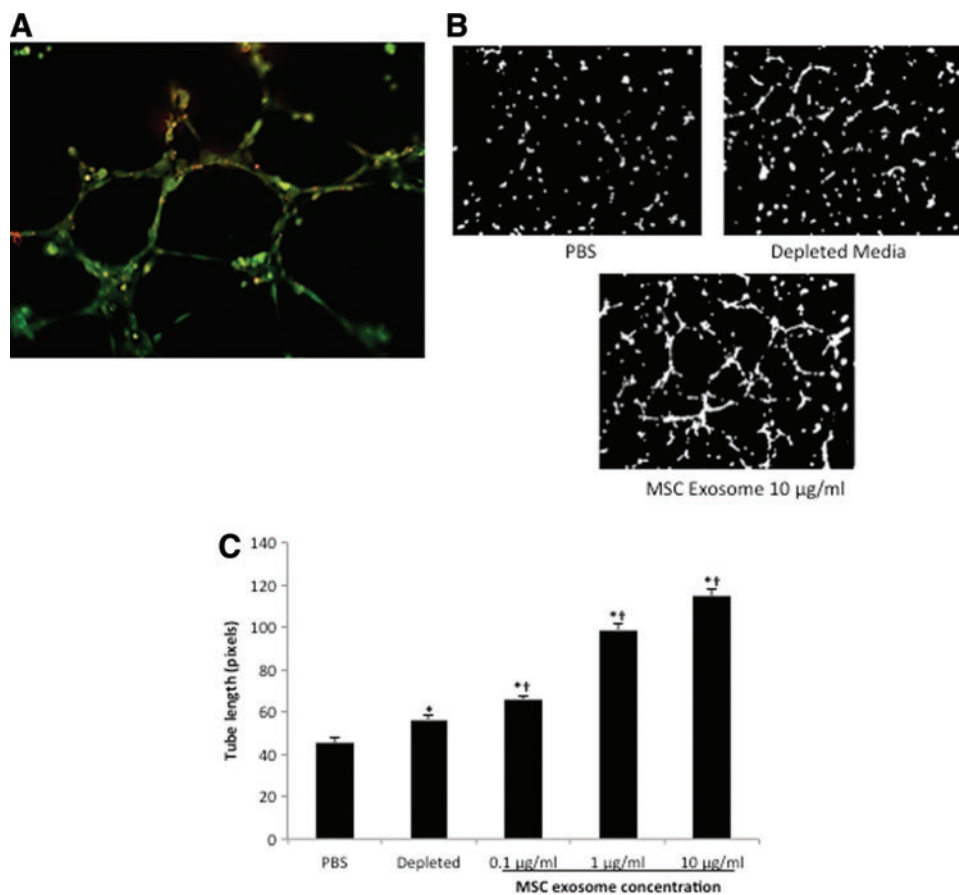

FIG. 5. MSC exosomes enhance angiogenesis in vitro. **(A)** PKH26-labeled MSC exosomes were added to human umbilical vein endothelial cells (HUVECs) for 6 h. After incubation with exosomes, cells were washed thrice and stained with Calcein AM. Numerous PKH26-labeled MSC exosomes (*red*) were observed within the branching network of HUVECs (*green*). **(B)** Micrographs showing effect of MSC exosomes on tube formation by HUVECs. HUVECs (5 × 104/well) were incubated for 6 h at 37°C on Geltrex substratum in the presence of the indicated dose of MSC exosomes. The cells were stained with Calcein AM and imaged. **(C)** Bar graph showing quantification of tube formation in the presence of vehicle, depleted medium, and increasing concentration of MSC exosomes. Tube-forming assay was performed as described, and the average tube length in pixels was quantified by ImagePro software. Triplicate results were averaged and mean ± SEM is shown. MSC exosome treated HUVECs showed significant and dose-dependent effects on the amount of tube formation compared with vehicle and depleted medium. *$P < 0.05$ versus vehicle; †$P < 0.05$ versus depleted conditioned medium. Pairwise one-tailed Student's *t*-tests was used for statistical analysis. Color images available online at www.liebertpub.com/scd
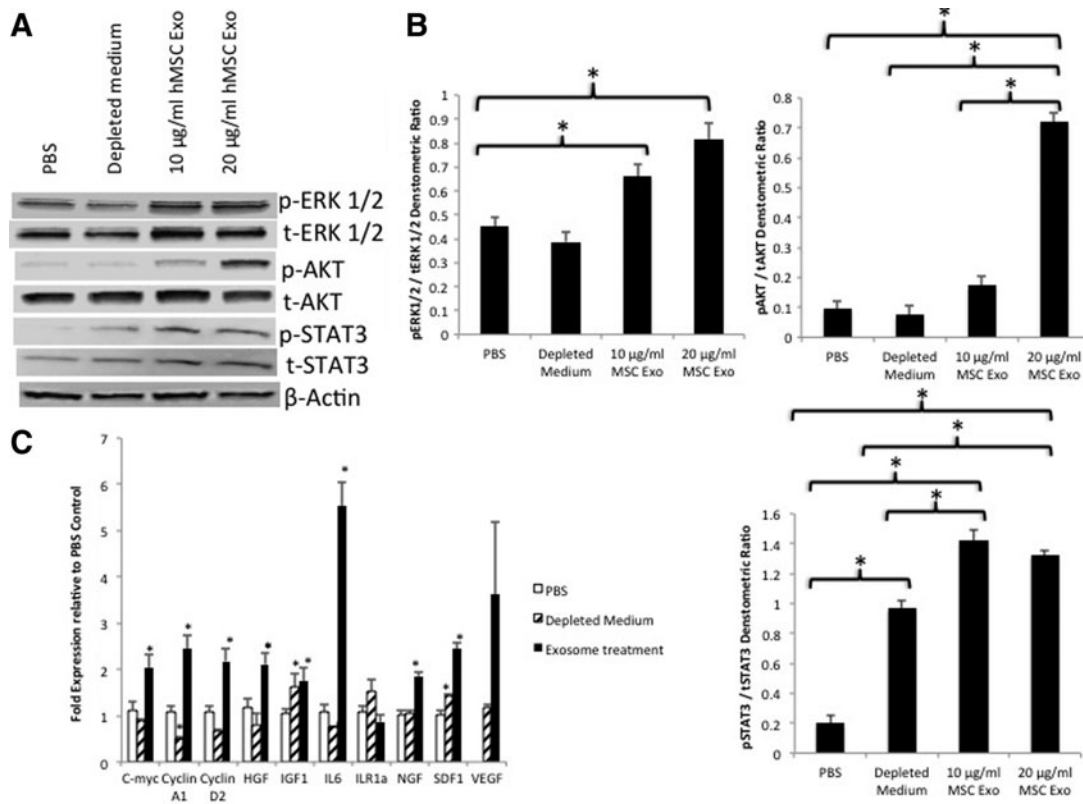
FIG. 6. MSC exosomes activate trophic signaling pathways and gene expression. **(A)** Normal adult fibroblasts were plated in six-well plates (10^5 cells per well). After overnight starvation, cells were exposed to vehicle, depleted medium, or MSC exosomes (10 or 20 μg/mL) for 2 h. After these treatments, total extracts were prepared and analyzed by western blotting for phosphoStat3 (Tyr705) and total Stat3, phospho AKT (Ser473) and total AKT, and phospho ERK 1/2 (Thr202/204) and total ERK 1/2, and β-actin protein levels. **(B)** Densitometry of the signaling pathways. Densitometry analysis was performed in triplicate and one-way analysis of variance with Bonferroni's post hoc test was used for analysis. *$P < 0.05$. **(C)** Gene expression analysis by qRT-PCR using glyceraldehyde 3-phosphate dehydrogenase (GAPDH) as the reference gene. *$P < 0.05$ versus PBS control. Triplicate results were averaged and mean ± SEM is shown. HGF, hepatocyte growth factor; IGF1, insulin growth factor-1; IL-6, interleukin-6; ILRA1, interleukin receptor antagonist-1; NGF, nerve growth factor; qRT-PCR, quantitative real-time polymerase chain reaction; SDF1, stromal derived growth factor-1; VEGF, vascular endothelial growth factor.

vehicle, depleted medium, or MSC exosomes (10 or 20 μg/mL) for 2 h. Figure 6A (with densitometry shown in Fig. 6B) shows significant activation of Akt (phosphorylation of Ser473) and STAT3 (phosphorylation of Thr705) along with enhanced signaling of ERK 1/2 (phosphorylation of Thr202/204) after MSC exosome treatment.

As the activation of these signaling pathways, particularly STAT3, is known to induce the expression of a number of genes, including those involved in cell cycle progression and growth factor production, we used qRT-PCR to quantify expression of cell cycle, growth factor, and cytokine genes. After serum starvation overnight, cells were treated with MSC exosomes or vehicle for 24 h. Figure 6C reveals there was a significant induction in genes involved in cell cycle progression (c-myc, cyclin A1, and cyclin D2), growth factors [hepatocyte growth factor (HGF), insulin-like growth factor-1 (IGF1), nerve growth factor (NGF), and stromal-derived growth factor-1 (SDF1)] and the cytokine interleukin-6 (IL-6). Although, the induction vascular endothelial growth factor (VEGF) was not statistically significant, there was a trend toward increased expression ($P = 0.078$). There was no difference in the expression of interleukin receptor antagonist-1 between exosome treatment and PBS. In con-

trast, depleted medium showed only significant increases in IGF1 and SDF1.

MSC exosomes are enriched with STAT3 that is transcriptionally active

STAT3 plays an important role in normal wound healing and response to injury [39]. Furthermore, STAT3 signaling controls a wide array of cellular processes, including cellular proliferation, migration, and angiogenesis by targeting the expression of many genes such as those involved in cell cycle control (c-myc and cyclin) and encoding cytokines and growth factors (IL-6, HGF, and VEGF) [40–42]. Given that MSC exosomes were able to enhance fibroblast proliferation and migration, enhance tube formation of HUVECs and increase a number of STAT3 genes, we next examined whether MSC exosomes contained STAT3. Figure 7A clearly demonstrate the presence of STAT3 and STAT3 phosphorylated at Thr705 in exosomes isolated from MSCs. Next, we assessed whether exosomal STAT3 had DNA-binding activity utilizing an ELISA-based STAT3–DNA binding assay. Indeed, exosomal STAT3 did demonstrate DNA-binding activity (Fig. 7B).
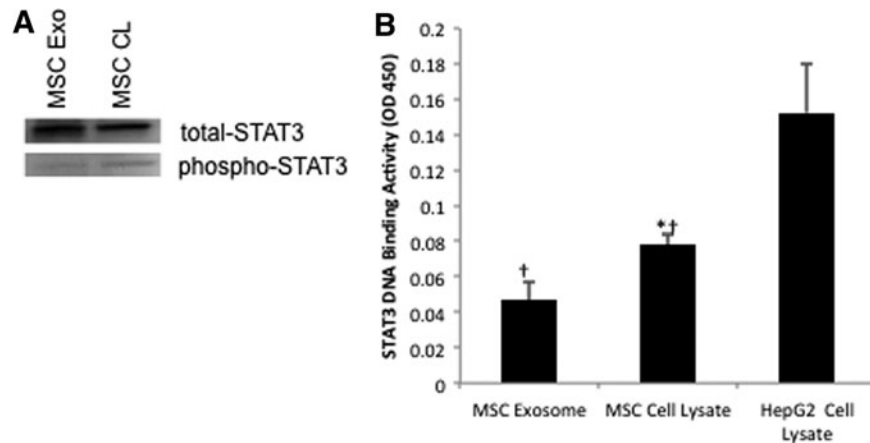
FIG. 7. MSC exosomes contain Stat3. **(A)** Twenty micrograms MSC exosome and cellular extract preparations were loaded into the respective lane and analyzed by western blotting for phosphoTyr705 and total Stat3. **(B)** Cellular and exosomal extracts (10 μg) were assayed for STAT3 DNA-binding activity using the TransAM kit per manufacturer's instructions. All results were normalized by subtraction of background controls Quantitative data in figure are presented as mean ± SEM of triplicate samples. HepG2 cell lysate (HepG2 CL) was used as a positive control. *$P < 0.05$ versus MSC exosome. $^{†}P < 0.05$ versus HepG2 Cell lysate. Pairwise one-tailed Student's t-tests was used for statistical analysis.

Discussion

Bone marrow-derived MSCs have been shown to be efficacious in the treatment of wounds, including chronic wounds [14,18,19]. Previous work in our laboratory has demonstrated that bone marrow-derived cells play an important role in cutaneous wound healing and that direct application of bone marrow-derived cells to patients with chronic nonhealing wounds leads to wound closure and dermal rebuilding [43–47].

It was originally thought MSCs homed to injured tissue, differentiated, and replaced damaged tissue, however, subsequent studies have shown that MSC engraftment and differentiation to injured sites are low and transient [48]. Instead, it is believed that MSCs exert their therapeutic effects through secreted paracrine or trophic factors [15–17]. Experiments utilizing MSC-conditioned media have demonstrated the importance of the paracrine mechanism of BM-MSC-induced wound healing [49–52]. More recent work in our laboratory has demonstrated that MSCs could enhance fibroblast migration without cell contact in a dose-dependent manner [19].

It has been demonstrated that eukaryotic cells possess highly sophisticated membrane trafficking mechanisms to mediate cellular communication. For example, it has been reported that cells cultured in vitro exchange information by shedding MVs and form tunneling nanotubes [53]. Indeed, we were able to demonstrate that MSCs cocultured with fibroblasts formed ultrafine intracellular structures resembling tunneling nanotubes that connect the cytoplasm of distantly located cells. We also noticed the release and uptake of MVs by MSCs in coculture.

Exosomes, a type of MV are produced by fusion of the multivesicular body with the plasma membrane, and are released from and taken up by most cell types [20–22]. In our study, we successfully isolated MSCs exosomes, confirmed their smooth spherical shape resembling a lipid bilayer structure and verified the expression of exosomal marker proteins CD9, CD63, CD81, Alix, Tsg101, and flottilin-1.

Exosomes have recently gained attention as being the possible paracrine mediators of MSCs in several disease models. Results so far have indicated that these exosomes may be important in reducing myocardial infarction size, protecting against acute tubular injury, promoting functional recovery after stroke, and ameliorating inflammation after Escherichia coli endotoxin-induced acute lung injury [54–57]. We subsequently hypothesized that MSC exosomes could also mediate the effects of wound healing attributed to MSCs observed in our recent studies.

Dermal fibroblasts provide critical functions during wound healing, including wound contraction, extracellular matrix deposition, and tissue remodeling. Fibroblasts from chronic wounds are defective in their ability to migrate, proliferate, and secrete growth factors [58–60].

Our experiments found that fluorescently labeled MSC exosomes were uptaken by fibroblasts and that they could enhance the growth and migration of normal and diabetic chronic wound fibroblasts in a dose-dependent fashion. Furthermore, we found that MSC exosomes were uptaken by HUVECs and enhanced endothelial angiogenesis in vitro. This latter finding is in line with several reports demonstrating the angiogenic potential of MSC-conditioned medium [61–63], and a recent report by Bian et al. that examined the angiogenic effects of MSC exosomes [64].

MSC-conditioned medium includes cytokines such as IL-6, IGF1, VEGF, and basic fibroblast growth factor [65–67]. Yet, numerous clinical studies of recombinant growth factors used to treat chronic wounds have reported disappointing results [68]. Proteolytic degradation of growth factors and unresponsive growth factor signaling cascades are thought to contribute to an impaired wound healing response [69,70]. Interestingly, consistent with those results, we found that cellular proliferation, migration, and angiogenesis were significantly impaired when the conditioned medium was depleted of exosomes by ultracentrifugation.

Exosomes produced by MSCs would be expected to have several advantages in the wound environment. Their lipid bilayer shell could avert proteolytic degradation and thus

more effectively transfer signals to target cells (eg, fibroblasts and endothelial cells). In addition, exosomes contain many potential regulatory components including miRNAs, mRNAs, and proteins, which can be transferred as a type of "physiological lipofection" to recipient cells to modify their characteristics [71]. This ability to transfer complex messages could explain evidence in previously described experiments where cellular extracts were found to induce epigenetic changes in recipient cells. For example, fibroblasts after exposure to lymphatic cell extracts express genes typical for lymphocytes [72] and similarly, hematopoietic stem cells exposed to the extracts from damaged liver cells began to express genes specific for hepatocytes [73]. Exosomes likely accomplish these changes by exerting a direct effect on specific pathways in recipient cells. Dovrat et al. found that β-catenin was secreted in extracellular vesicles and could activate the WNT pathway in recipient cells [74]. MSC exosomes have been found to transfer growth factor receptor mRNA, which was translated to the corresponding protein in renal tubular cells [75].

Also important in wound healing is that MSC exosomes appear to induce changes by activation of growth factor signaling cascades. We have demonstrated that MSC exosomes activate important signaling cascades in target cells, including AKT, STAT3, and ERK. By stimulating these pathways, target cells would increase their expression of a number of growth factors, namely HGF, IL-6, IGF1, NGF, and SDF1. Further, we also postulate that the release of these factors may induce autocrine activation of additional signaling cascades, possibly accounting the activation of additional signaling cascades, including AKT and ERK 1/2, and further activation of STAT3. Activation of these signaling cascades with increased growth factor and growth factor receptor production is particularly relevant, as chronic wounds have attenuated signaling cascades and growth factor expression.

Given STAT3's important role in wound healing, including roles in migration, proliferation, angiogenesis, and growth factor production [37], we examined whether MSC exosomes carry STAT3. To our surprise, we found that MSC exosomes did indeed carry STAT3, which also had DNA-binding activity. Although, elucidating the exact role of exosomal STAT3 requires further study, we speculate it may be in part responsible for transcription of genes involved in our study, including Cyclin D2, c-myc, HGF, VEGF, and IL-6, which are known to be transcriptionally activated by STAT3 [39]. Future work will be required to delineate the exact role of exosomal STAT3 in relation to activation of STAT3 signaling in the target cell.

In conclusion, we found that MSC exosomes could enhance the growth and migration of normal and chronic wound fibroblasts, and induce angiogenesis in vitro. Furthermore, we demonstrate that MSC exosomes contained transcriptionally active STAT3 and MSC exosomes were able to activate AKT, ERK 1/2, and STAT3 and induce the expression of a number of trophic factors. We hypothesize that exosomes derived from MSCs could be used for wound healing as a safe and effective "off the shelf" product and possibly obviate the concerns of MSCs, including transfer of infectious agents, development of unwanted cell types, culture-induced senescence, loss of functional properties, genetic instability, and/or eventual malignant transformation [76].

Author Disclosure Statement

No competing financial interests exist.

References

1. Sen CK, GM Gordillo, S Roy, R Kirsner, L Lambert, TK Hunt, F Gottrup, GC Gurtner and MT Longaker. (2009). Human skin wounds: a major and snowballing threat to public health and the economy. Wound Repair Regen 17: 763–771.
2. Mustoe TA, K O'Shaughnessy and O Kloeters. (2006). Chronic wound pathogenesis and current treatment strategies: a unifying hypothesis. Plast Reconstr Surg 117: 35S–41S.
3. Velnar T, T Bailey and V Smrkolj. (2009). The wound healing process: an overview of the cellular and molecular mechanisms. J Int Med Res 37:1528–1542.
4. Robson MC, DL Steed and MG Franz. (2001). Wound healing: biologic features and approaches to maximize healing trajectories. Curr Probl Surg 38:72–140.
5. Baum CL and CJ Arpey. (2005). Normal cutaneous wound healing: clinical correlation with cellular and molecular events. Dermatol Surg 31:674–686; discussion 686.
6. Galiano RD, OM Tepper, CR Pelo, KA Bhatt, M Callaghan, N Bastidas, S Bunting, HG Steinmetz and GC Gurtner. (2004). Topical vascular endothelial growth factor accelerates diabetic wound healing through increased angiogenesis and by mobilizing and recruiting bone marrow-derived cells. Am J Pathol 164:1935–1947.
7. Brem H and M Tomic-Canic. (2007). Cellular and molecular basis of wound healing in diabetes. J Clin Invest 117: 1219–1222.
8. Lerman OZ, RD Galiano, M Armour, JP Levine and GC Gurtner. (2003). Cellular dysfunction in the diabetic fibroblast: impairment in migration, vascular endothelial growth factor production, and response to hypoxia. Am J Pathol 162:303–312.
9. Loots MA, EN Lamme, JR Mekkes, JD Bos and E Middelkoop. (1999). Cultured fibroblasts from chronic diabetic wounds on the lower extremity (non-insulin-dependent diabetes mellitus) show disturbed proliferation. Arch Dermatol Res 291:93–99.
10. Fahey TJ, 3rd, A Sadaty, WG Jones, 2nd, A Barber, B Smoller and GT Shires. (1991). Diabetes impairs the late inflammatory response to wound healing. J Surg Res 50: 308–313.
11. Prockop DJ. (1997). Marrow stromal cells as stem cells for nonhematopoietic tissues. Science 276:71–74.
12. Uccelli A, L Moretta and V Pistoia. (2008). Mesenchymal stem cells in health and disease. Nat Rev Immunol 8:726–736.
13. Jackson WM, LJ Nesti and RS Tuan. (2012). Concise review: clinical translation of wound healing therapies based

on mesenchymal stem cells. Stem Cells Transl Med 1: 44–50.

14. Hanson SE, ML Bentz and P Hematti. (2010). Mesenchymal stem cell therapy for nonhealing cutaneous wounds. Plast Reconstr Surg 125:510–516.

15. Shabbir A, D Zisa, M Leiker, C Johnston, H Lin and T Lee. (2009). Muscular dystrophy therapy by nonautologous mesenchymal stem cells: muscle regeneration without immunosuppression and inflammation. Transplantation 87: 1275–1282.

16. Shabbir A, D Zisa, H Lin, M Mastri, G Roloff, G Suzuki and T Lee. (2010). Activation of host tissue trophic factors through JAK-STAT3 signaling: a mechanism of mesenchymal stem cell-mediated cardiac repair. Am J Physiol Heart Circ Physiol 299:H1428–H1438.

17. Shabbir A, D Zisa, G Suzuki and T Lee. (2009). Heart failure therapy mediated by the trophic activities of bone marrow mesenchymal stem cells: a noninvasive therapeutic regimen. Am J Physiol Heart Circ Physiol 296:H1888–H1897.

18. Chen L, EE Tredget, PY Wu and Y Wu. (2008). Paracrine factors of mesenchymal stem cells recruit macrophages and endothelial lineage cells and enhance wound healing. PLoS One 3:e1886.

19. Rodriguez-Menocal L, M Salgado, D Ford and E Van Badiavas. (2012). Stimulation of skin and wound fibroblast migration by mesenchymal stem cells derived from normal donors and chronic wound patients. Stem Cells Transl Med 1:221–229.

20. Vlassov AV, S Magdaleno, R Setterquist and R Conrad. (2012). Exosomes: current knowledge of their composition, biological functions, and diagnostic and therapeutic potentials. Biochim Biophys Acta 1820:940–948.

21. Camussi G, MC Deregibus, S Bruno, V Cantaluppi and L Biancone. (2010). Exosomes/microvesicles as a mechanism of cell-to-cell communication. Kidney Int 78:838–848.

22. Valadi H, K Ekstrom, A Bossios, M Sjostrand, JJ Lee and JO Lotvall. (2007). Exosome-mediated transfer of mRNAs and microRNAs is a novel mechanism of genetic exchange between cells. Nat Cell Biol 9:654–659.

23. Aga M, GL Bentz, S Raffa, MR Torrisi, S Kondo, N Wakisaka, T Yoshizaki, JS Pagano and J Shackelford. (2014). Exosomal HIF1alpha supports invasive potential of nasopharyngeal carcinoma-associated LMP1-positive exosomes. Oncogene.

24. Roccaro AM, A Sacco, P Maiso, AK Azab, YT Tai, M Reagan, F Azab, LM Flores, F Campigotto, et al. (2013). BM mesenchymal stromal cell-derived exosomes facilitate multiple myeloma progression. J Clin Invest 123:1542–1555.

25. Théry C, S Amigorena, G Raposo and A Clayton. (2006). Isolation and characterization of exosomes from cell culture supernatants and biological fluids. Curr Protoc Cell Biol Chapter 3:Unit 3 22.

26. Hosseini-Beheshti E, S Pham, H Adomat, N Li and ES Tomlinson Guns. (2012). Exosomes as biomarker enriched microvesicles: characterization of exosomal proteins derived from a panel of prostate cell lines with distinct AR phenotypes. Mol Cell Proteomics 11:863–885.

27. Chambers AE, PF Stanley, H Randeva and S Banerjee. (2011). Microvesicle-mediated release of soluble LH/hCG receptor (LHCGR) from transfected cells and placenta explants. Reprod Biol Endocrinol 9:64.

28. Yang L, XH Wu, D Wang, CL Luo and LX Chen. (2013). Bladder cancer cell-derived exosomes inhibit tumor cell apoptosis and induce cell proliferation in vitro. Mol Med Rep 8:1272–1278.

29. Shifrin DA, Jr., M Demory Beckler, RJ Coffey and MJ Tyska. (2013). Extracellular vesicles: communication, coercion, and conditioning. Mol Biol Cell 24:1253–1259.

30. Stewart K, P Monk, S Walsh, CM Jefferiss, J Letchford and JN Beresford. (2003). STRO-1, HOP-26 (CD63), CD49a and SB-10 (CD166) as markers of primitive human marrow stromal cells and their more differentiated progeny: a comparative investigation in vitro. Cell Tissue Res 313: 281–290.

31. Gutierrez-Vazquez C, C Villarroya-Beltri, M Mittelbrunn and F Sanchez-Madrid. (2013). Transfer of extracellular vesicles during immune cell-cell interactions. Immunol Rev 251:125–142.

32. Camacho L, P Guerrero and D Marchetti. (2013). Micro-RNA and protein profiling of brain metastasis competent cell-derived exosomes. PLoS One 8:e73790.

33. van Balkom BW, OG de Jong, M Smits, J Brummelman, K den Ouden, PM de Bree, MA van Eijndhoven, DM Pegtel, W Stoorvogel, T Wurdinger and MC Verhaar. (2013). Endothelial cells require miR-214 to secrete exosomes that suppress senescence and induce angiogenesis in human and mouse endothelial cells. Blood 121:3997–4006, S1–S15.

34. Sohel MM, M Hoelker, SS Noferesti, D Salilew-Wondim, E Tholen, C Looft, F Rings, MJ Uddin, TE Spencer, K Schellander and D Tesfaye. (2013). Exosomal and non-exosomal transport of extra-cellular microRNAs in follicular fluid: implications for bovine oocyte developmental competence. PLoS One 8:e78505.

35. Liang CC, AY Park and JL Guan. (2007). In vitro scratch assay: a convenient and inexpensive method for analysis of cell migration in vitro. Nat Protoc 2:329–333.

36. Squarize CH, RM Castilho, TH Bugge and JS Gutkind. (2010). Accelerated wound healing by mTOR activation in genetically defined mouse models. PLoS One 5:e10643.

37. Sano S, KS Chan and J DiGiovanni. (2008). Impact of Stat3 activation upon skin biology: a dichotomy of its role between homeostasis and diseases. J Dermatol Sci 50:1–14.

38. Sharma GD, J He and HE Bazan. (2003). p38 and ERK1/2 coordinate cellular migration and proliferation in epithelial wound healing: evidence of cross-talk activation between MAP kinase cascades. J Biol Chem 278:21989–21997.

39. Dauer DJ, B Ferraro, L Song, B Yu, L Mora, R Buettner, S Enkemann, R Jove and EB Haura. (2005). Stat3 regulates genes common to both wound healing and cancer. Oncogene 24:3397–3408.

40. Funamoto M, Y Fujio, K Kunisada, S Negoro, E Tone, T Osugi, H Hirota, M Izumi, K Yoshizaki, et al. (2000). Signal transducer and activator of transcription 3 is required for glycoprotein 130-mediated induction of vascular endothelial growth factor in cardiac myocytes. J Biol Chem 275:10561–10566.

41. Wojcik EJ, S Sharifpoor, NA Miller, TG Wright, R Watering, EA Tremblay, K Swan, CR Mueller and BE Elliott. (2006). A novel activating function of c-Src and Stat3 on HGF transcription in mammary carcinoma cells. Oncogene 25:2773–2784.

42. Huang WL, HH Yeh, CC Lin, WW Lai, JY Chang, WT Chang and WC Su. (2010). Signal transducer and activator of transcription 3 activation up-regulates interleukin-6 autocrine production: a biochemical and genetic study of es-

tablished cancer cell lines and clinical isolated human cancer cells. Mol Cancer 9:309.

43. Badiavas EV and V Falanga. (2003). Treatment of chronic wounds with bone marrow-derived cells. Arch Dermatol 139:510–516.

44. Badiavas AR and EV Badiavas. (2011). Potential benefits of allogeneic bone marrow mesenchymal stem cells for wound healing. Expert Opin Biol Ther 11:1447–1454.

45. Badiavas EV. (2004). The potential of bone marrow cells to orchestrate homeostasis and healing in skin. Blood Cells Mol Dis 32:21–23.

46. Badiavas EV, M Abedi, J Butmarc, V Falanga and P Quesenberry. (2003). Participation of bone marrow derived cells in cutaneous wound healing. J Cell Physiol 196: 245–250.

47. Badiavas EV, D Ford, P Liu, N Kouttab, J Morgan, A Richards and A Maizel. (2007). Long-term bone marrow culture and its clinical potential in chronic wound healing. Wound Repair Regen 15:856–865.

48. Kean TJ, P Lin, AI Caplan and JE Dennis. (2013). MSCs: Delivery Routes and Engraftment, Cell-Targeting Strategies, and Immune Modulation. Stem Cells Int 2013: 732742.

49. Jun EK, Q Zhang, BS Yoon, JH Moon, G Lee, G Park, PJ Kang, JH Lee, A Kim and S You. (2014). Hypoxic conditioned medium from human amniotic fluid-derived mesenchymal stem cells accelerates skin wound healing through TGF-beta/SMAD2 and PI3K/Akt pathways. Int J Mol Sci 15:605–628.

50. Tamama K and SS Kerpedjieva. (2012). Acceleration of wound healing by multiple growth factors and cytokines secreted from multipotential stromal cells/mesenchymal stem cells. Adv Wound Care (New Rochelle) 1:177–182.

51. Tamari M, Y Nishino, N Yamamoto and M Ueda. (2013). Acceleration of wound healing with stem cell-derived growth factors. Int J Oral Maxillofac Implants 28:e369–e375.

52. Walter MN, KT Wright, HR Fuller, S MacNeil and WE Johnson. (2010). Mesenchymal stem cell-conditioned medium accelerates skin wound healing: an in vitro study of fibroblast and keratinocyte scratch assays. Exp Cell Res 316:1271–1281.

53. Rustom A, R Saffrich, I Markovic, P Walther and HH Gerdes. (2004). Nanotubular highways for intercellular organelle transport. Science 303:1007–1010.

54. Lai RC, F Arslan, MM Lee, NS Sze, A Choo, TS Chen, M Salto-Tellez, L Timmers, CN Lee, et al. (2010). Exosome secreted by MSC reduces myocardial ischemia/reperfusion injury. Stem Cell Res 4:214–222.

55. Bruno S, C Grange, MC Deregibus, RA Calogero, S Saviozzi, F Collino, L Morando, A Busca, M Falda, et al. (2009). Mesenchymal stem cell-derived microvesicles protect against acute tubular injury. J Am Soc Nephrol 20: 1053–1067.

56. Xin H, Y Li, Y Cui, JJ Yang, ZG Zhang and M Chopp. (2013). Systemic administration of exosomes released from mesenchymal stromal cells promote functional recovery and neurovascular plasticity after stroke in rats. J Cereb Blood Flow Metab 33:1711–1715.

57. Zhu YG, XM Feng, J Abbott, XH Fang, Q Hao, A Monsel, JM Qu, MA Matthay and JW Lee. (2014). Human mesenchymal stem cell microvesicles for treatment of Escherichia coli endotoxin-induced acute lung injury in mice. Stem Cells 32:116–125.

58. Brem H, MS Golinko, O Stojadinovic, A Kodra, RF Diegelmann, S Vukelic, H Entero, DL Coppock and M Tomic-Canic. (2008). Primary cultured fibroblasts derived from patients with chronic wounds: a methodology to produce human cell lines and test putative growth factor therapy such as GMCSF. J Transl Med 6:75.

59. Greives MR, F Samra, SC Pavlides, KM Blechman, SM Naylor, CD Woodrell, C Cadacio, JP Levine, TA Bancroft, et al. (2012). Exogenous calreticulin improves diabetic wound healing. Wound Repair Regen 20:715–730.

60. Wall IB, R Moseley, DM Baird, D Kipling, P Giles, I Laffafian, PE Price, DW Thomas and P Stephens. (2008). Fibroblast dysfunction is a key factor in the non-healing of chronic venous leg ulcers. J Invest Dermatol 128:2526–2540.

61. Wang CY, HB Yang, HS Hsu, LL Chen, CC Tsai, KS Tsai, TL Yew, YH Kao and SC Hung. (2012). Mesenchymal stem cell-conditioned medium facilitates angiogenesis and fracture healing in diabetic rats. J Tissue Eng Regen Med 6:559–569.

62. Guiducci S, M Manetti, E Romano, B Mazzanti, C Ceccarelli, S Dal Pozzo, AF Milia, S Bellando-Randone, G Fiori, et al. (2011). Bone marrow-derived mesenchymal stem cells from early diffuse systemic sclerosis exhibit a paracrine machinery and stimulate angiogenesis in vitro. Ann Rheum Dis 70:2011–2021.

63. Oskowitz A, H McFerrin, M Gutschow, ML Carter and R Pochampally. (2011). Serum-deprived human multipotent mesenchymal stromal cells (MSCs) are highly angiogenic. Stem Cell Res 6:215–225.

64. Bian S, L Zhang, L Duan, X Wang, Y Min and H Yu. (2014). Extracellular vesicles derived from human bone marrow mesenchymal stem cells promote angiogenesis in a rat myocardial infarction model. J Mol Med (Berl) 92:387–397.

65. Kinnaird T, E Stabile, MS Burnett, CW Lee, S Barr, S Fuchs and SE Epstein. (2004). Marrow-derived stromal cells express genes encoding a broad spectrum of arteriogenic cytokines and promote in vitro and in vivo arteriogenesis through paracrine mechanisms. Circ Res 94: 678–685.

66. Weil BR, TA Markel, JL Herrmann, AM Abarbanell and DR Meldrum. (2009). Mesenchymal stem cells enhance the viability and proliferation of human fetal intestinal epithelial cells following hypoxic injury via paracrine mechanisms. Surgery 146:190–197.

67. Zisa D, A Shabbir, G Suzuki and T Lee. (2009). Vascular endothelial growth factor (VEGF) as a key therapeutic trophic factor in bone marrow mesenchymal stem cell-mediated cardiac repair. Biochem Biophys Res Commun 390:834–838.

68. Robson MC. (1997). The role of growth factors in the healing of chronic wounds. Wound Repair Regen 5: 12–17.

69. Lauer G, S Sollberg, M Cole, I Flamme, J Sturzebecher, K Mann, T Krieg and SA Eming. (2000). Expression and proteolysis of vascular endothelial growth factor is increased in chronic wounds. J Invest Dermatol 115: 12–18.

70. Wu L, YP Xia, SI Roth, E Gruskin and TA Mustoe. (1999). Transforming growth factor-beta1 fails to stimulate wound healing and impairs its signal transduction in an aged ischemic ulcer model: importance of oxygen and age. Am J Pathol 154:301–309.

71. Fleissner F, Y Goerzig, A Haverich and T Thum. (2012). Microvesicles as novel biomarkers and therapeutic targets in transplantation medicine. Am J Transplant 12:289–297.

72. Hakelien AM, HB Landsverk, JM Robl, BS Skalhegg and P Collas. (2002). Reprogramming fibroblasts to express T-cell functions using cell extracts. Nat Biotechnol 20:460–466.

73. Jang YY, MI Collector, SB Baylin, AM Diehl and SJ Sharkis. (2004). Hematopoietic stem cells convert into liver cells within days without fusion. Nat Cell Biol 6:532–539.

74. Dovrat S, M Caspi, A Zilberberg, L Lahav, A Firsow, H Gur and R Rosin-Arbesfeld. (2014). 14-3-3 and beta-catenin are secreted on extracellular vesicles to activate the oncogenic Wnt pathway. Mol Oncol 8:894–911.

75. Tomasoni S, L Longaretti, C Rota, M Morigi, S Conti, E Gotti, C Capelli, M Introna, G Remuzzi and A Benigni. (2013). Transfer of growth factor receptor mRNA via exosomes unravels the regenerative effect of mesenchymal stem cells. Stem Cells Dev 22:772–780.

76. Wu Y, S Huang, J Enhe and X Fu. (2012). Insights into bone marrow-derived mesenchymal stem cells safety for cutaneous repair and regeneration. Int Wound J 9:586–594.

Address correspondence to:
Dr. Evangelos Van Badiavas
Department of Dermatology and Cutaneous Surgery
Interdisciplinary Stem Cell Institute
University of Miami Miller School of Medicine
1600 NW 10th Avenue
RBSB 2023A
Miami, FL 33136

E-mail: ebadiavas@med.miami.edu